Modeling electric potential and salinity gradient-driven ion transport through nanochannels

10.585 Course Project

Gaurav Awasthi
First-year PhD student, Department of Chemical Engineering, MIT

Abstract

Nanochannels in general present exciting opportunities for improved separation, water desalination, and energy conversion applications due to the high energy power density in the transport of fluid and ions across these conduits[1]. An interest in nanofluidic osmotic energy conversion systems has been sparked by advances in nanofabrication technologies, as well as new computational and experimental methods to probe these systems[2]. The driving potentials used differ based on the application. Here, we study the effects of size and cross-sectional shape of nanochannels on ionic transport through them under an external potential and under a concentration gradient. Specifically, the ionic current and power generation are studied. It is observed that while the cross-section of a nanochannel does not significantly influence the current under an external potential, the length of the nanochannel does strongly influence it. We further observe that an "average radius" approximation for nanotubes of varying cross-sections does not fit well within the ionic transport model described by Cui et al.[1] and Emmerich et al[3].

Introduction

Ion-exchange membranes are thin, selective membranes that allow specific ions (e.g., H^+ or Na^+) to pass through while blocking others. They are widely used in desalination, fuel cells, and energy generation, with applications extending to drug delivery and biosensors. Developing nanopores and nanofluidic membranes with improved ion transport properties for applications is essential for improving power generation performance[4]. Osmotic energy is acknowledged as a sustainable form of "blue" energy and originates from the salt gradient present between freshwater and saline solutions, such as seawater and industrial wastewater[5]. The rational design of nanomembranes for these applications necessitates complete understanding of the transport dynamics through nanochannels.

Flow at the nano-scale differs significantly from bulk flow due to several reasons. Firstly, there are confinement effects because molecules are constrained to move dimensions comparable to their mean free paths. Secondly, the increased dominance of surface effects due to a high surface-to-volume ratio makes surface properties like charge and roughness very important. This further results in slipping at the walls, a phenomenon generally neglected at the bulk scale. The breakdown of continuum approximations, enhanced transport properties, and the formation of an electric double layer leads to unique behavior, especially when considering ionic transport. Cui et al.[1] present an analysis of salinity-driven flow through a double-walled carbon nanotube (DWCNT) with a circular cross-section and length of the order of 100 μm. Choi et al.[6] analyze electric

potential driven pore-blocking current through a single-walled carbon nanotube, and also attempt to reconcile their work with a theoretical model. Emmerich et al.[3] study electric potential and salinity gradient-driven flow through pristine graphene and activated carbon nanoconduits with a rectangular cross-section with lengths of the order of a few μm. The relevant electrochemical transport theory and some parameter values are also available in literature[3,6,7]. Additional theoretical analysis is succinctly presented by Sebastian & Green[8] and by Lavi & Green[9] by drawing an analogy between the flow through the nanochannel and the current flow through a resistive electric circuit.

1. Electric potential driven flow

As described by Choi et al., the net ionic transport is due to the general motion of charged ions through an electric field (produced by the potential difference) and due to convective fluid transport through the nanochannel. They study the current at different concentrations of a KCl solution. In an "open pore" condition, the current is purely due to the motion of protons and hydroxide ions, and the current is expressed as

(1) $I_{open} = eE(\mu_H C_H^{open} - \mu_{OH} C_{OH}^{open}) + e\bar{v}(C_H^{open} - C_{OH}^{open})$

Here, *e* is the electronic charge, E the electric field due to the potential difference, μ is the mobility of the ion, $\bar{v}$ is the average fluid velocity, and C_H^{open} and C_H^{closed} are the number of protons per unit length in the tube. Due to the negative charge on the nanotube, the current can be approximated as only being due to the protons, and the equation simplifies to:

(2) $I_{open} = eE(\mu_H C_H^{open}) + e\bar{v}(C_H^{open})$

The entrance of a larger K^+ ion decreases the concentration of protons in the nanochannel, and the "closed-pore" current is described as $I_{closed} = e\bar{v}_b(C_H^{closed})$. Here the current reduces to purely convective transport at a reduced velocity. The authors mention that the value of C_H^{open} and C_H^{closed} (concentration of protons per unit length) are difficult to calculate experimentally, but can be approximated as the surface charge density (with appropriate units) of the nano-conduit as electric neutrality must be maintained. The average velocity (for open and closed pores respectively) required for both the equations can be calculated from the enhanced transport equations:

(3) $32\nu_0 \frac{\eta(D)}{\epsilon(D)} = 4\frac{eC_H^o E_f}{\pi}\left(\frac{\mu_H(D)E_f}{\nu^b} + 1\right)$

(4) $32\nu^b \frac{\eta(D)}{\epsilon(D)} = 4\frac{eC_H^o E_f}{\pi}\left(\frac{\mu_H(D)E_f}{\nu^b}\right)$

It is important to note that the mobility is also diameter dependent, as described in equation S6 of Choi et al. as $\mu_H(D) = \mu_H^{bulk}\left(1 + 39exp\left(-\frac{D - 0.81nm}{0.33nm}\right)\right)$. The pore blocking current is further calculated as $I_{open} - I_{closed}$.

2. Salinity gradient driven flow

The works by Cui et al.[1] and Emmerich et al.[3] use nanochannels of varying cross-sections, shapes, and materials, and apply the same transport models for salinity conductance. This model was proposed by Mouterde et al.[10] and is derived by considering how the surface charges change the hydrodynamic boundary conditions. The diffusion-osmotic mobility further derived accounts for the surface conductance as well. As mentioned in both the works, we know that

$$I_{osm} = \frac{area}{length} K_{osm} \log\left(\frac{C_{max}}{C_{min}}\right) \quad (5)$$

$$K_{osm} = \frac{1}{2}\frac{(-2\Sigma)k_B T}{h 2\pi\eta l_B}\left(1 - \frac{sinh^{-1}\chi}{\chi} + (1-\alpha_{ion})\frac{b_0}{\lambda_D}\frac{\sqrt{1+\chi^2}-1}{1+\beta_s\frac{|\Sigma|}{e}l_B^2}\right) \quad (6)$$

where the prefactor of ½ applies to activated surfaces only. The parameters are all defined in Table 1.

Parameter	**Physical relevance**
e	Electronic charge
l_B	Bjerrum length
λ_D	Debye length
χ	Dimensionless, see following equation
b_0	Slip length
ϵ	Permittivity of material
Σ	Surface charge
β_s	Friction between water molecules and surface
α_{ion}	Friction between mobile ions and surface

Table 1: Physical meaning of parameters appearing in equation (6)

The expressions for some of the parameters are:

$$(6.1)\ l_B = \frac{e^2}{4\pi\epsilon k_B T}$$

$$(6.2)\ \chi = 2\pi\lambda_D l_B \frac{\Sigma}{e}$$

$$(6.3)\ \lambda_D = (8\pi l_B C_s)^{-1/2}$$

We also know that the maximum power $P = \frac{I_{osm}^2}{4G}$, where the channel conductance G is derived from the I-V curve at each concentration ratio. The theoretical formula for G from Siria et al.[11] is

$$(7)\ G = 2e^2\mu C_s \frac{\pi R^2}{L} + e\mu\frac{2\pi R}{L}|\Sigma|(1+\chi).$$

We can replace πR^2 by the cross-sectional area and $2\pi R$ by the perimeter of the desired conduit with a differing geometry.

Results and Discussion

1. Electric potential driven flow

We first attempt to replicate the pore-blocking current mentioned in Choi et al. by taking a cylindrical single-walled ultra-long carbon nanotube of diameter 2 nm. The parameters used are the same as in the original study, except the values of C_H^{open} and C_H^{closed} were not explicitly mentioned. We approximate $C_H^{closed} = 2\pi \frac{D}{e} \Sigma$ by considering the surface charge Σ on an activated carbon nanotube given in Section 4.1 of the Supplementary Information of Emmerich et al. C_H^{open} was varied parametrically to get the best fit and was finally chosen as $1.2\, C_H^{closed}$. The figure below shows a good agreement between the model predictions against the replication data (R2 > 0.93).

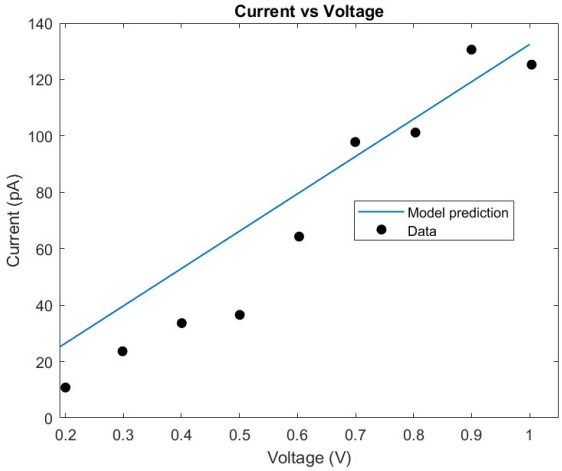

Fig 1. Replication of Choi et al. results

The experiments by Emmerich et al. were performed on rectangular nanoconduits of length scales ~ 10 microns, almost 100x smaller than those considered by Choi et al. It is not immediately apparent that the model will be valid given the different bulk resistances to flow, the relative importance of entrance effects (the energetic barrier to a charge carrier entering the nanotube) and any potential effects due to the shape of the nanochannel. We consider two systems here: (1) width 100 nm, height 3 nm, length 10 microns made of activated carbon, and (2) width 120 nm, height 3 nm, length 9.6 microns made of pristine graphene. Since the equations are derived for cylindrical nanochannels, we use the width and height of the Emmerich et al. nanochannels to find the "hydraulic diameter" as 4*area/perimeter. The code was written in MATLAB v. R2024A. A comparison of the model predictions, actual data, and R^2 values for activated and pristine channels are all presented in Fig 2 and Table 2. We see that while the model is more accurate for activated channels, it is not a particularly good fit in either case, possibly due to a combination of the reasons above. The relatively worse fit for pristine channels is probably due to the fewer mobile charges on the graphene surface, which further leads to much lower surface conductivity (almost two

orders of magnitude lower than activated channels). In both cases, the solid line represents the model fit and the circle markers represent the data from Fig 2a and 2e of Emmerich et al., with each color representing a different concentration.

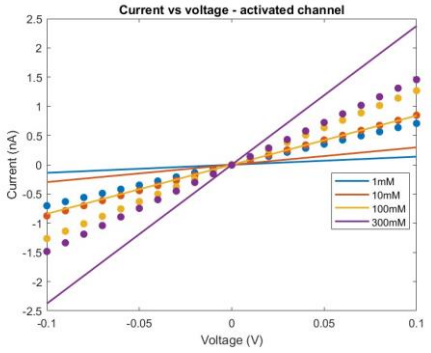

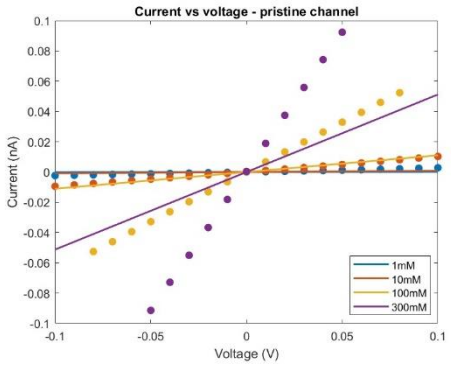

Concentration (mM)	R^2 value
1	0.35
10	0.57
100	0.89
300	0.62

Concentration (mM)	R^2 value
1	0.06
10	0.17
100	0.31
300	0.48

Fig 2. Application of model to Emmerich et al. data for (a) activated (b) pristine channels

Table 2. R^2 values for different concentrations (a) activated (b) pristine channels

We attempt to simplify our analysis by testing each assumption individually by considering hypothetical systems similar to the original system presented in Choi et al.

a. *Ultra-long rectangular nanochannel with hydraulic diameter = 2 nm*
   With this hypothetical system, the only difference is the shape of the channel, and the width and height are specifically selected to yield a hydraulic diameter that matches the original cylindrical diameter. Applying the model to this system, and comparing with the data from Choi et al., we see a fit that is comparable to the original replication data, indicating that our hydraulic diameter approximation is indeed valid. Further, these results suggest that the deviation observed in the previous figure were due to the relevant importance of entrance effects and bulk resistance, or, in other words, the length scales of the nanotube.

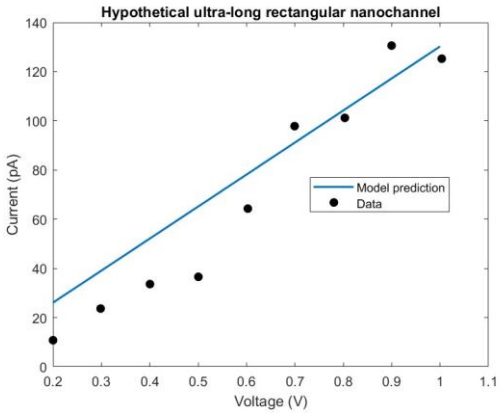

Fig 3. Hypothetical system with same length as Choi et al. data

b. *Accounting for entrance effects*

To account for the relative importance of entrance effects in the shorter nanotubes, we introduce an entrance resistance defined by Sebastian et al.[8] as $R_{access} = \frac{\rho_{electrolyte}}{4r_{cylinder}}$. This access resistance arises due to the energy barrier that an ion experiences when approaching the nanotube. Since this resistance can be considered to be in series with the existing bulk resistance of the channel, we model the new net current as

(8) $$I = \frac{V}{R_{total}} = \frac{V}{\frac{V}{I_{closed}} + R_{access}}$$

Note that we only desire an order of magnitude estimate here, and so we only account for We see that incorporating the access resistance leads to good improvement, especially for higher concentrations. In Fig 4. the solid line shows the original model, and the dotted line shows the model accounting for the access resistance. The resistivity of the solution is lower at higher concentrations of KCl, and we see the fit significantly improving for those higher concentrations. This indicates that accounting for access resistance is at least a step in the right direction, and more sophisticated models for the entrance resistance can be considered to improve the model across concentration ranges.

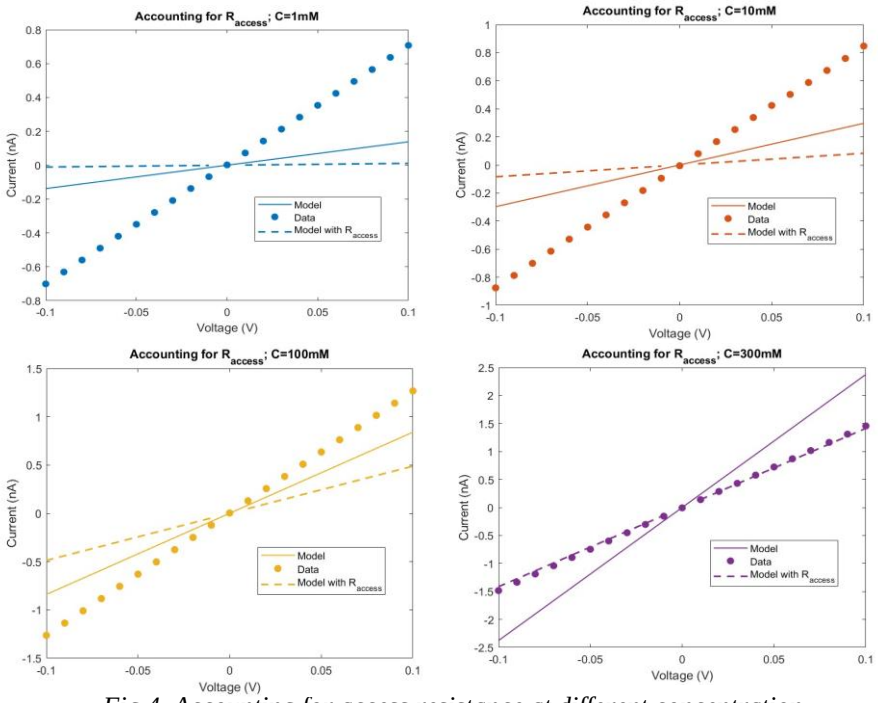

Fig 4. Accounting for access resistance at different concentration

2. Salinity gradient driven flow

Both Cui et al. and Emmerich et al. use the same model for concentration gradient-driven flow despite varying the nanochannel shape (cylindrical in the former, rectangular in the latter), indicating that the model is valid across geometries. We attempt to fit the model to computational study by Li et al.[12] that simulates flow through a cylindrical nanochannel with a sinusoidally varying radial cross-section. The study attempts to model the inherent surface irregularities introduced when fabricating nanochannels by modeling them as a sinusoid. Finite-element methods are used to solve the Navier-Stokes, Nernst-Planck and Poisson equations simultaneously. The authors further compare the osmotic current and power generated by the flow induced by a KCl concentration gradient for various channel lengths. Using an average radius of 15 nm as mentioned by the authors, we attempt to fit the model[10] to this system at varying lengths and analyze the goodness-of-fit. A schematic of the system is reproduced from Li et al. in Fig 5., and the results are summarized in Table 3 and Figure 6.

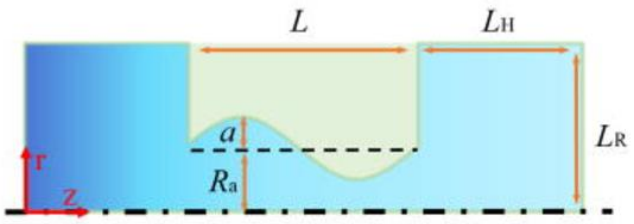

Fig 5. Schematic of sinusoidally varying nanochannel, reproduced from Fig 1(b) of Li et al.[12]

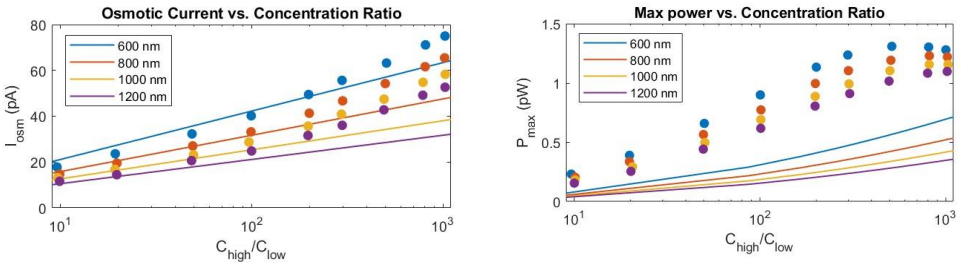

Fig 6. Comparison of model[10] and Li et al. data (solid line: model prediction, circle: data)

Length (nm)	R^2 (for current)
600	0.91
800	0.71
1000	0.59
1200	0.34

Table 3. R^2 values for current at different nanotube lengths

Conclusion

Four systems (single-walled CNT, pristine graphene rectangular nanochannel, activated carbon rectangular nanochannel, and sinusoidally varying nanochannel) were compared across two driving force conditions (electric potential and salinity gradient). All the nanoconduits compared had varying cross-sectional areas and lengths. This work investigated the validity of models proposed in the literature across nanochannels of varying cross-sections and length scales with the overall aim of contributing to efforts towards rational design of efficient membranes for separation and osmotic power generation.

In the case of electric potential-driven flow, we see that calculating a "hydraulic diameter" is infact suitable for simplifying the analysis of non-cylinder cross-sections, even though the hydraulic diameter is term generally associated with bulk turbulent flows. We further see that the Choi et al. model applies better to ultra-long nanotubes and does not fit well at shorter lengths, however, accounting for access resistance is a promising step to understand transport through shorter nanochannels. The model is also more accurate at higher concentration of charge carriers, and works better for systems with mobile surface charges. These results can be used to optimize nanochannel design for separation applications. To further theoretical analysis, shape and material-specific access resistance formulations have been developed and can be used.

In the case of salinity gradient-driven flow, we see that the shape of the nanochannel is seen to be a strong determinant of the osmotic current and power generation. The model described by Mouterde et al.[10] is shown to apply better for lower concentration gradients and shorter channels. We also notice that sinusoidally-varying channels are shown to have 2-3x greater power generation capacity than cylindrical channels of similar dimensions, and that increasing channel length decreases the power generated. A potential future direction for analysis is to replace the fixed surface charge density with one varying with pH, solution concentration, temperature etc. All in

all, these results can inform rational nanochannel design for osmotic power generation applications.

Data availability

All of the data used in this work has been obtained from publicly available, peer-reviewed literature. All the materials needed for the analysis have been uploaded to Github and are accessible here.

Appendix

Estimation of Parameters

1. Surface charge density
   Σ was linearly interpolated from the values present in Supplementary Section 4.1 of Emmerich et al.[3]
2. C_H^{open} and C_H^{closed} in equation (1)
   By rescaling the units of the surface charge density found from to the desired units of number of protons per unit length, we obtain $C_H^{closed} = 2\pi \frac{D}{e} \Sigma$
3. C_s in equation 6
   This parameter represents the concentration of electrolyte within the tube, and was estimated as the average of the concentration at the two tube ends, ie, $\frac{C_{high} + C_{low}}{2}$
4. $\rho_{resistivity}$ in the formulation for access resistance
   The resistivity of seawater (0.5 M NaCl) is known to be 0.2 Ω-m[13], and the resistivities at the desired concentrations were linearly estimated from this known value.

References

(1) Cui, G.; Xu, Z.; Li, H.; Zhang, S.; Xu, L.; Siria, A.; Ma, M. Enhanced Osmotic Transport in Individual Double-Walled Carbon Nanotube. *Nat. Commun.* **2023**, *14* (1), 2295. https://doi.org/10.1038/s41467-023-37970-3.

(2) Zhang, Z.; Wen, L.; Jiang, L. Nanofluidics for Osmotic Energy Conversion. *Nat. Rev. Mater.* **2021**, *6* (7), 622–639. https://doi.org/10.1038/s41578-021-00300-4.

(3) Emmerich, T.; Vasu, K. S.; Niguès, A.; Keerthi, A.; Radha, B.; Siria, A.; Bocquet, L. Enhanced Nanofluidic Transport in Activated Carbon Nanoconduits. *Nat. Mater.* **2022**, *21* (6), 696–702. https://doi.org/10.1038/s41563-022-01229-x.

(4) Tong, X.; Liu, S.; Crittenden, J.; Chen, Y. Nanofluidic Membranes to Address the Challenges of Salinity Gradient Power Harvesting. *ACS Nano* **2021**, *15* (4), 5838–5860. https://doi.org/10.1021/acsnano.0c09513.
(5) Li, S.; Wang, J.; Lv, Y.; Cui, Z.; Wang, L. Nanomaterials-Based Nanochannel Membrane for Osmotic Energy Harvesting. *Adv. Funct. Mater.* **2024**, *34* (4), 2308176. https://doi.org/10.1002/adfm.202308176.
(6) Choi, W.; Ulissi, Z. W.; Shimizu, S. F. E.; Bellisario, D. O.; Ellison, M. D.; Strano, M. S. Diameter-Dependent Ion Transport through the Interior of Isolated Single-Walled Carbon Nanotubes. *Nat. Commun.* **2013**, *4* (1), 2397. https://doi.org/10.1038/ncomms3397.
(7) Mouterde, T.; Keerthi, A.; Poggioli, A. R.; Dar, S. A.; Siria, A.; Geim, A. K.; Bocquet, L.; Radha, B. Molecular Streaming and Its Voltage Control in Ångström-Scale Channels. *Nature* **2019**, *567* (7746), 87–90. https://doi.org/10.1038/s41586-019-0961-5.
(8) Sebastian, J.; Green, Y. Electrical Circuit Modeling of Nanofluidic Systems. *Adv. Phys. Res.* **2023**, *2* (10), 2300044. https://doi.org/10.1002/apxr.202300044.
(9) Lavi, O.; Green, Y. A Theoretical Characterization of Osmotic Power Generation in Nanofluidic Systems. *Commun. Mater.* **2024**, *5* (1), 1–7. https://doi.org/10.1038/s43246-024-00559-4.
(10) Mouterde, T.; Bocquet, L. Interfacial Transport with Mobile Surface Charges and Consequences for Ionic Transport in Carbon Nanotubes. *Eur. Phys. J. E* **2018**, *41* (12), 148. https://doi.org/10.1140/epje/i2018-11760-2.
(11) Siria, A.; Poncharal, P.; Biance, A.-L.; Fulcrand, R.; Blase, X.; Purcell, S. T.; Bocquet, L. Giant Osmotic Energy Conversion Measured in a Single Transmembrane Boron Nitride Nanotube. *Nature* **2013**, *494* (7438), 455–458. https://doi.org/10.1038/nature11876.
(12) Li, C. (李昌铮); Li, Z. (李振全); Zhang, Z. (张哲); Qiao, N. (乔楠); Liao, M. (廖梦振). Salinity Gradient Power Generation in Sinusoidal Nanochannels. *Phys. Fluids* **2024**, *36* (2), 022007. https://doi.org/10.1063/5.0186962.
(13) *The Resistivity Of Water Explained*. Atlas Scientific. https://atlas-scientific.com/blog/resistivity-of-water/ (accessed 2024-12-12).